Collagen Induces Anisotropy in Fingertip Subcutaneous Tissues During Contact

Duprez Guillaume H.C., Delhaye Benoit P., Delannay Laurent

***Abstract*—The subcutaneous mechanical response of the fingertip is highly anisotropic due to the presence of a network of collagen fibers linking the outer skin layer to the bone. The impact of this anisotropy on the fingerpad deformation, which had not been studied until now, is here demonstrated using a two-dimensional finite element model of a transverse section of the finger. Different distributions of fiber orientations are considered: radial (physiologic), circumferential, and random (isotropic). The three variants of the model are assessed using experimental observations of a finger pressed on a flat surface. Predictions relying on the physiological orientation of fibers best reproduce experimental trends. Our results show that the orientation of fibers significantly influences the distribution of internal strains and stresses. This leads to a sudden change in the profile of contact pressure when transitioning from sticking to slipping. Interpreted in terms of tactile perception or sensation, these variations might represent important sensory cues for partial slip detection. This is also valuable information for the development of haptic devices.**

***Index Terms*—Finite Element Modeling, Hyperelastic, Tactile, Sense of touch**

I. Introduction

When grasping objects or exploring surfaces, our perception of touch is ensured by biological sensors, called *tactile mechanoreceptors*, which densely innervate the fingertips [1]. The related neuronal activity may be probed under a large variety of stimuli (see for review [1], [2]). However, it remains unclear which information exactly is communicated to the brain. One of the important challenges in the interpretation of mechano-transduction is that afferents are embedded at some depth (from $\sim$500 μm to several mm) inside the finger pad and they hence witness subcutaneous strains which are likely to differ from those observed along the skin outer surface [3].

Various modeling approaches have aimed to simulate the deformation of a finger pressed on a flat surface. Analytical solutions have been derived for the simplest loading scenarios, by considering that the finger is either a frictionless elastic half-space (Boussinesq problem) [4]–[6], or an elastic membrane filled with an incompressible fluid (waterbed model), which better predicts surface deflection under line load [7]. Some more realistic simulations were achieved using the finite element method, allowing to study the behavior of the fingertip when loaded by complex indenters [8]. The response of the soft biological tissues was then most often considered linear elastic (assumption of infinitesimal strains), sometimes accounting for the multilayered structure of the skin in 2D [9] or in 3D [10]. Some even considered the topology of the fingerprint [11]. Only a few studies [12], [13] assumed a hyperelastic material behavior which allows a mathematically rigorous account of the non-linear response of physiological tissues under finite isochoric deformation [14]. Most of the past studies involved monotonic loadings but a small number of them did consider the fingertip response under oscillatory loads. The propagation of vibrations inside the soft tissues in a fingertip has been analyzed both in 2D [9] and 3D [15]. The vibration modes of the fingertip have also been estimated [16].

All of the latter studies assumed an isotropic material response, disregarding the fact that the network of collagen fibers, which is hosted by subcutaneous tissues, is likely to induce significant anisotropy. Indeed histological observations have evidenced that collagen fibers are not randomly distributed [17]. They rather are "radially" aligned: one fiber end is anchored on the bone and the other end comes close to reaching the skin. If the deformation of the fingertip is such that some collagen fibers are stretched, these fibers are expected to sustain high tensile stresses along their axis [18]. The famous Holzapfel-Gasser-Ogden (i.e., HGO) hyperelastic model [19] accounts for the asymmetry of the fiber response under compressive and tensile axial loads. It also predicts the anisotropic macroscopic response resulting from the preferential alignment of the collagen fiber network, and it fulfills volume preservation as expected in soft biological tissues [20].

G. Duprez and L. Delannay are with the Institute of Mechanics, Materials and Civil Engineering, UCLouvain, 1348 Louvain-la-Neuve, Belgium

B. Delhaye is with the Institute of Information and Communication Technologies, Electronics and Applied Mathematics, UCLouvain, 1348 Louvain-la-Neuve, Belgium

The present study aims to assess to which extent the anisotropy induced by the radial network of collagen fibers is likely to influence the deformation of a finger pressed on a flat surface as well as the build-up of internal stresses and the pressure distribution along the surface of contact. The finite element model described in Section II is used for the simulation of laboratory experiments presented in Section III. The results are shown in Section IV and they are discussed in Section V, before the conclusion.

II. Description of the numerical model

The simulations involve a finger pressed on a horizontal plate which is considered perfectly flat and infinitely stiff. This is a fair assumption as the plate used in experiments (Fig. 1(a-b)) is made of glass. Fig. 1(c) defines the characteristic dimensions of the finger ellipsoidal cross-section. Contact with the plate is established by prescribing a vertical displacement (along $\hat{e}_y$) to the bone, assuming that only the surrounding subcutaneous tissues can deform. In the simulations, it being performed in 2D, the contact area A is deduced from the contact width W and is assumed circular $A = \pi \frac{W^2}{4}$. The error induced by this approximation is estimated using image analysis software ImageJ [22]. As shown in Fig. 1(b), this assumption results in an underestimation of the gross contact area by approximately 9.5% when the contact angle is $\sim 30°$. Friction is simulated by displacing the bone along the horizontal direction $\hat{e}_x$ while maintaining a fixed amplitude of the vertical contact force. The Coulomb coefficient for friction is assumed constant and its value is determined (in Section IV) based on experimental measurements of the ratio between the tangential (horizontal) and normal (vertical) contact forces.

Quasi-static simulations are carried out using Abaqus/Standard 2021 [23] (*Simulia, Dassault Systèmes*,

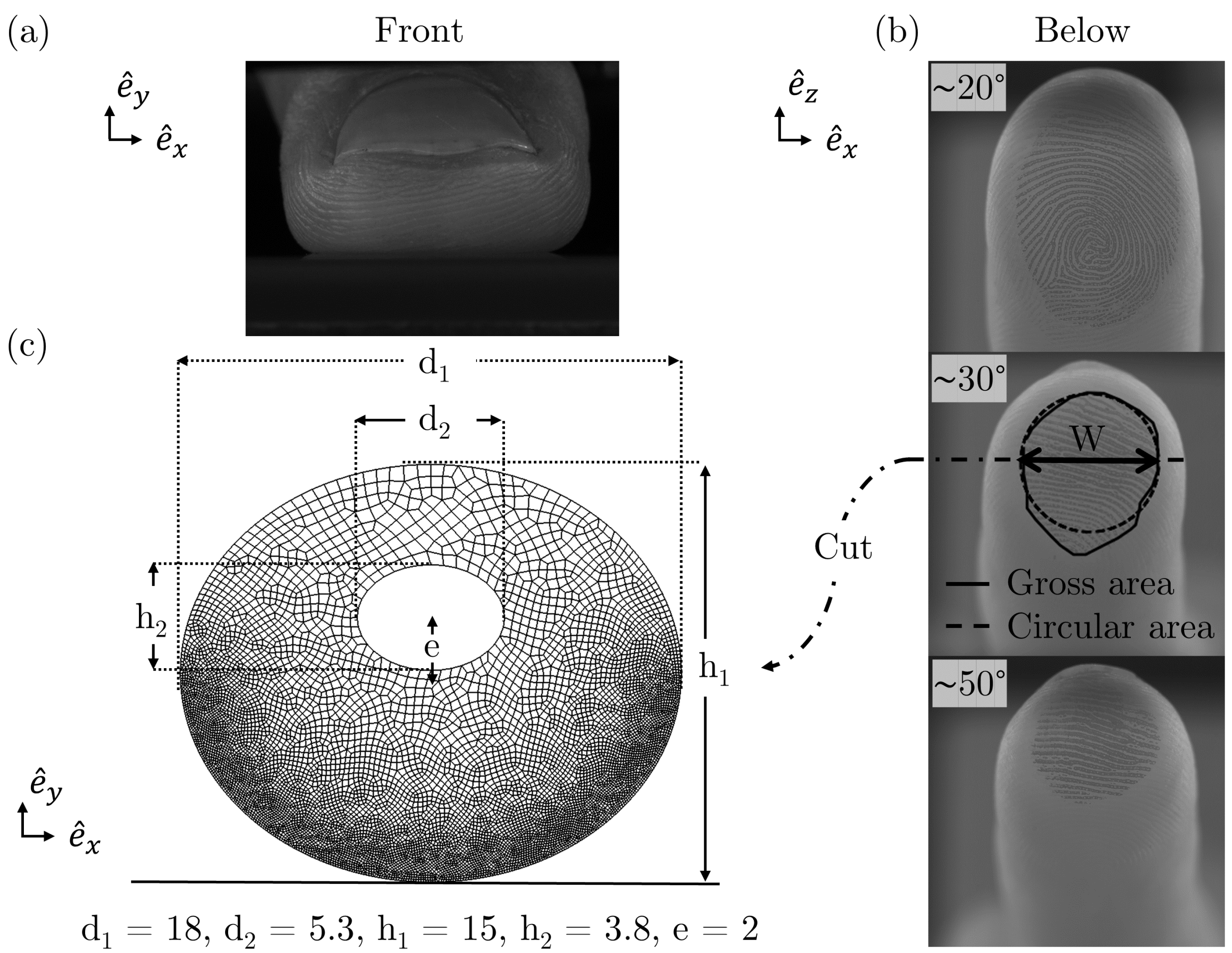

Fig. 1. 2D modeling of a cross-section of the fingertip. Fingertip compression against a glass plate under $\sim$5 N normal load as seen from the front (a), or from below (b) at different angles of attack. Images are obtained using the apparatus presented in [21]. (c) Finite element mesh with characteristic dimensions.

France) finite element (FE) solver. The FE mesh is generated using the gmsh suite [24], and the element size is refined in the region which comes in contact with the rigid plate (Fig. 1(c)). Generalized plane-strain conditions are adopted, which means that deformation is considered uniform along the out-of-plane direction $\hat{e}_z$. Simulations are performed twice using different values of the out-of-plane stiffness. Four-node hybrid elements are used to overcome the numerical issues (locking, see [25]) which may arise when a material undergoes finite strains under constant volume. This implies that the hydrostatic stress is computed at every location of the mesh as a Lagrange multiplier enforcing zero divergence in the displacement field (according to the weak formulation of the mechanical equilibrium equations, which is typical of FE solutions [25]).

Inside the subcutaneous tissues, a significant increase of stiffness is expected when collagen fibers are stretched in the course of the loading. The latter is accounted for by relying on the HGO anisotropic hyperelastic model [19]. If we consider that, at any location across the FE mesh, collagen fibers are precisely aligned along N directions (no local dispersion relative to these directions), the hyperelastic strain-energy density function W of the HGO model may be expressed as

$$\mathrm{W} = \mathrm{c}(\bar{\mathrm{I}}_1 - 3) + \frac{\mathrm{k}_1}{2\mathrm{k}_2} \sum_{\alpha=1}^{\mathrm{N}} \left[\exp\left(\mathrm{k}_2 \langle \lambda_\alpha^2 - 1 \rangle^2 \right) - 1 \right] \tag{1}$$

Here conventional denominations are used: the parameters c and k_1 are stiffnesses representative of, respectively, the isotropic ground matrix of the subcutaneous tissues and the collagen fibers, whereas k_2 is dimensionless and determines the rate of increase of the stiffness when collagen fibers are stretched. The scalar variable $\bar{\mathrm{I}}_1 = \mathrm{tr}(\overline{\mathbf{C}})$ is the first invariant of the isochoric part of the right Cauchy-Green strain tensor $\overline{\mathbf{C}} = \mathrm{J}^{\frac{-2}{3}}\mathbf{C}$ where $\mathbf{C} = \mathbf{F}^{\mathrm{T}}\mathbf{F}$ and $\mathbf{F}$ is the deformation gradient tensor. The scalar variable $\lambda_\alpha^2 = \mathbf{a}_\alpha \otimes \mathbf{a}_\alpha : \overline{\mathbf{C}}$ corresponds to the square of the stretch of the collagen fibers that are aligned with the unit vector $\mathbf{a}_\alpha$. As collagen fibers do not sustain compressive axial loads, the argument of the exponential is under Macaulay brackets: $\langle \mathrm{x} - 1 \rangle = \mathrm{x} - 1$ if $\mathrm{x} > 1$, and $\langle \mathrm{x} - 1 \rangle = 0$ otherwise.

In order to investigate the influence of the anisotropy induced by the collagen fibers on the deformation of the finger cross-section, three modeling hypotheses are tested regarding the fiber orientations. They are illustrated in Fig. 2(b-d). The first situation is the closest to the histological observations [17]: collagen fibers follow the shortest path from the bone to the skin, which is referred to as a *radial* network of fibers. The second situation treated is a fictitious one in which collagen fibers are aligned *circumferentially* around the bone. This unrealistic distribution of fibers is the most distant in regard to physiological observations. In the third set of simulations, the distribution of fibers is random so that the average response is *isotropic*. The latter is thus similar to previous studies in which the anisotropy induced by the collagen fibers was neglected.

In practice, the definition of appropriate fiber orientation(s) at every integration point of the FE mesh proceeds as follows:

- The "radial" network considers a single fiber orien-

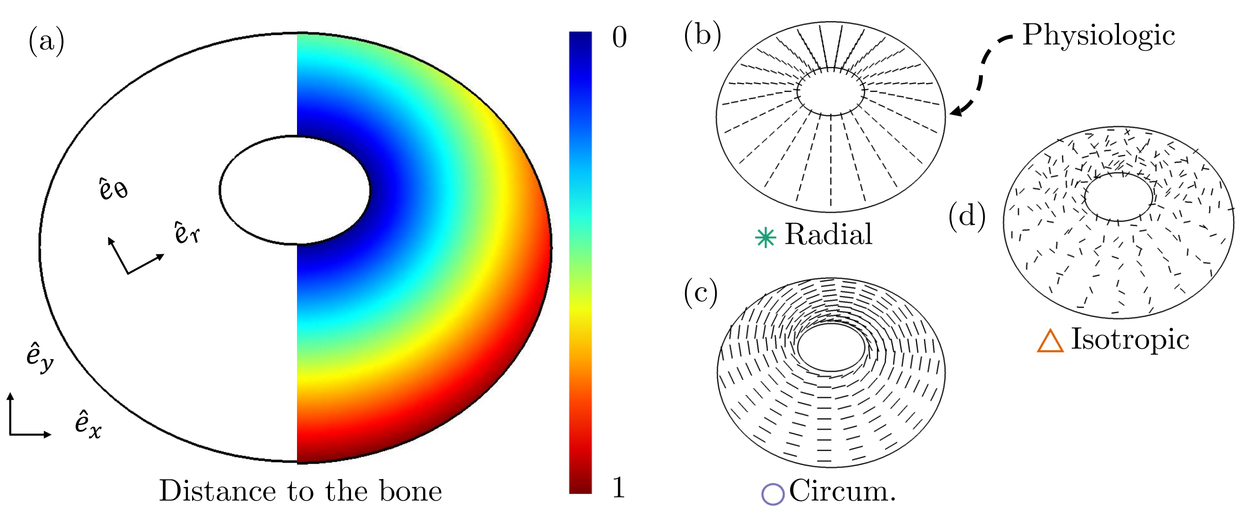

Fig. 2. Definition of the local orientation of collagen fibers in the 2D modeling of a fingertip section. (a) Gradient of the distance to the bone; (b) Radially oriented fibers; (c) Circumferentially oriented fibers; (d) Randomly oriented fibers yielding isotropic macroscopic behavior.

tation (N = 1) which corresponds to the shortest path to the inner ellipse (i.e., to the bone). The distance of each node of the mesh to the bone is thus computed and the unit "radial" vector ($\hat{e}_{\mathrm{r}}$ in Fig. 2 (a-b)) is computed based on the gradient of such distance field.
- The "circumferential" fiber orientations are defined inside the same cross-section, using the unit vector $\hat{e}_\theta$ which is perpendicular to $\hat{e}_{\mathrm{r}}$ as shown in Fig. 2(a,c). Here again, a single local orientation of collagen fibers is used at every integration point (N = 1).
- The isotropic response is obtained by considering three fiber orientations (N = 3) at every integration point. The first fiber orientation is selected randomly in the 2D section (Fig. 2(d)) and the other two orientations are tilted $+120°$ and $-120°$ relative to the first one. Such a definition of fiber orientations ensures isotropy and reduces noise.

III. Experimental data

Two sets of experimental observations of the deformation of a fingertip in contact with a glass plate [26], [27] are used to assess the predictions of the 2D FE model.

The first set of experimental measures focuses on the behavior of the fingertip under normal load [26]. A subject's index finger is pressed on a glass plate from 0 N to 2 N normal force at different angles of attack. Load-displacement data are recorded throughout the loading and the evolution of the contact area is estimated using ink prints of the fingertip at different load levels. The second set of experimental measures analyses the fingertip deformation under tangential loading [27]. The index is loaded with a glass plate up to a target normal force and the plate is then moved tangentially. The normal force and the angle of attack ($\pm 20°$) are fixed during the lateral displacement of the plate. Load-displacement data are measured and the evolution of the gross contact area is estimated by fitting the contour of the finger on the surface of the glass plate.

In the Results Section, the experiment labeled A refers to fingertip normal loading measurements made at an angle of attack of 30° as reported in [26]. Load-displacement and load-area data are extracted from the graphs in Fig. 3 and Fig. 5(a) in [26] using WebPlotDigitizer [28]. The data are then interpolated over the 0-2 N load range using the *interp1* function in Matlab [29] (*MathWorks*, United-States of America). Experiment B refers to fingertip tangential loading measurements made in [27]. Raw data collected at a sliding velocity of 10 mm/s in the radial and ulnar directions with a background normal force of 0.5 N are used. These two directions are chosen because they can be treated with the 2D FE model presented in Section 2. The sliding velocity is chosen arbitrarily, while 0.5 N is chosen as it falls in the range of spontaneous tactile exploration [30].

IV. Results

The 2D FE model is assessed based on a comparison of the predictions to experimental observations A and B (Fig. 3). To start, the parameters of the model are determined by ensuring that all three variants of the model reproduce the evolution of the contact force during fingertip normal loading through the vertical displacement of a plate (i.e., along $\hat{e}_{\mathrm{y}}$ in Fig. 1(a)) as measured in experiment A (Fig. 3(a)). The parameter for the isotropic ground matrix (i.e., c) is assigned a value independent of the orientation of the fiber. Similarly, the stiffening rate parameter for the collagen fibers (i.e., k_2) is assigned a constant value across all three variants. This ensures that both the ground matrix and the fibers exhibit consistent behavior in all variants. Only parameter k_1 is adapted when switching from one variant of the model to another. This parameter is proportional to the volume fraction of collagen fibers. The fit is enforced up to 0.5 N normal load and is done by trial and error while ensuring that the values of the parameters fall within the usual range when the HGO model is used to represent soft biological tissues. Experimental trends are properly reproduced up to 0.5 N when $\mathrm{k}_1 = 150$ kPa in the case of the radial fibers network, and when $\mathrm{k}_1 = 3$ kPa if the model relies on either the random or the circumferential fibers network. Parameters c and k_2 are set to, respectively, 3 kPa and 15. These values are within the usual range [19], [20], [33]. The model with radial fibers best reproduces the experimental measurements.

As Fig. 3(b) shows, in the case of normal loading, the three variants of the model lead to different predictions of the increase of the contact area as a function of the normal displacement. Among the three predictions, the experimental trend is best captured when the model assumes a radial network of collagen fibers. Fig. 3(b) also compares the predicted evolution of the contact area to the results of two existing models [31], [32]. These models, labeled Reference 1 and Reference 2, respectively simulate the normal loading of a fingertip pressed on a rigid plate at an angle of attack of $15°$ and $20°$, respectively. Both references account for a 3D multi-layered fingertip exhibiting isotropic hyperelastic behavior. In Reference 1 [31], force-displacement and force-area data for steel-finger contact are extracted from Fig. 3 using WebPlotDigitizer. The data are then interpolated over 0-2.5 mm plate displacement range

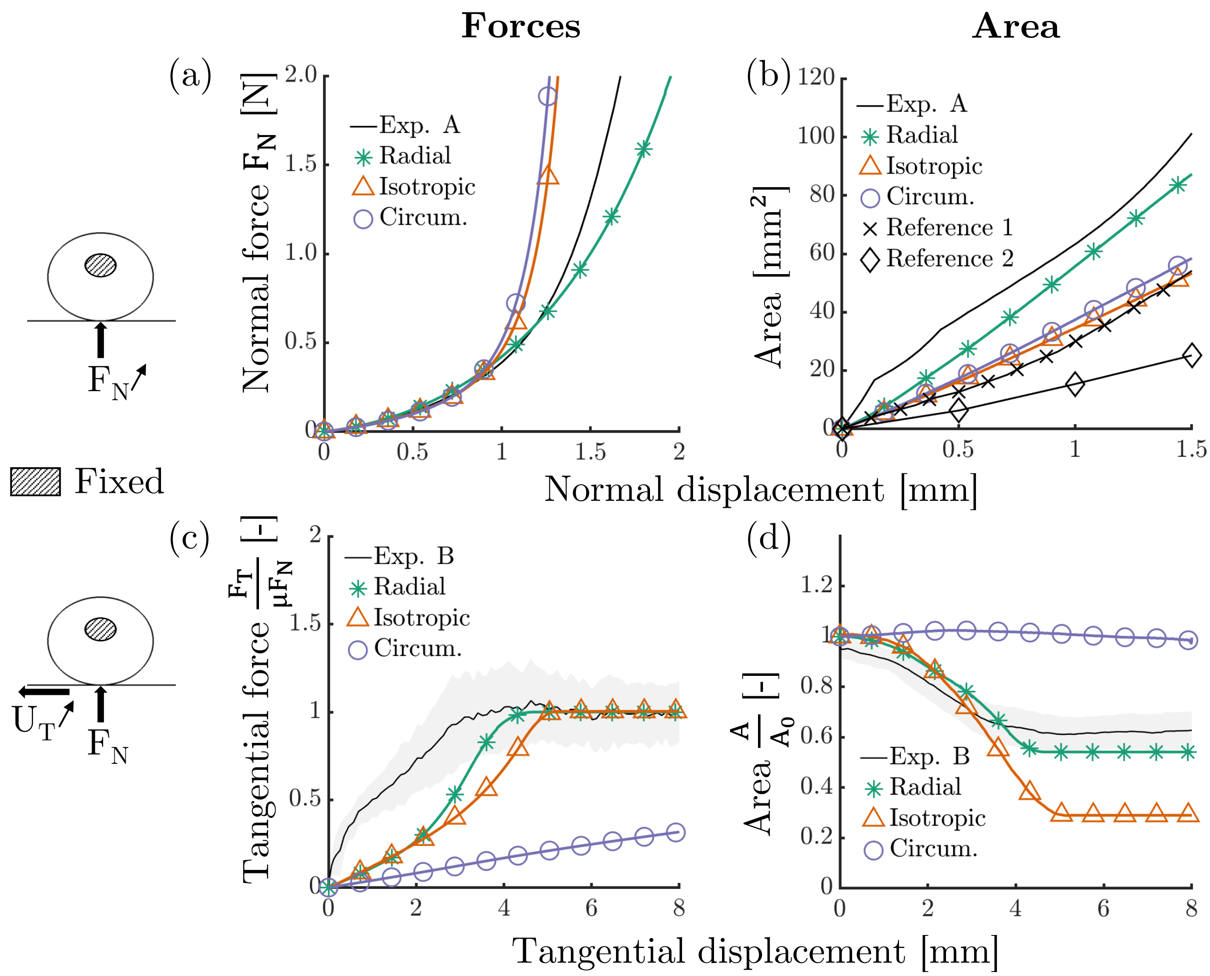

Fig. 3. Comparison of the numerical predictions with experimental data of fingertip normal and tangential loading (Exp. A [26] and Exp. B [27]) and against other 3D models (Reference 1 [31] and Reference 2 [32]). (a) Normal force F_N as a function of the vertical displacement of the plate; (b) Contact area A as a function of the vertical displacement of the plate; (c) Normalized tangential contact force F_T as a function of the tangential displacement of the plate; (d) Normalized contact area as a function of the tangential displacement of the plate.

using the *interp1* function in Matlab. In Reference 2 [32], the contact length L and the contact width W are available at 0.5, 1, and 1.5 mm of vertical plate displacement. These data points are extracted from Fig. 6 and Fig. 7 for the VH model in [32] using WebPlotDigitizer and an ellipsoid contact area is derived $A = \frac{\pi LW}{4}$. Fig. 3(b) shows that the variant with radial fibers best reproduces the experimental trend. The predictions by Reference 1 and Reference 2 are far below the measurements of experiment A.

The three variants of the model are now evaluated by simulating friction under tangential loading. As in experiment B, the normal component of the contact force is kept fixed at 0.5 N while a tangential displacement of 8 mm is applied. The friction coefficient is $\mu = 1$, which conforms to experimental measurements [34]. According to both the model and the experiment, both the tangential component of the force and the contact area evolve as function of the horizontal displacement of the bone. Both the force and the area maintain a constant value when fingertip sliding is initiated. In experiment B, the finger moved along either the ulnar or the radial direction (both under 0.5 N normal force). The average of the two measurements is used here in order to assess model predictions. The material parameters of the HGO model are identical to those used in the first set of simulations (which considered normal loading). In Fig. 3(c) the experimental and predicted tangential forces are normalized with respect to their respective sliding threshold. Fig. 3(d) depicts the corresponding evolution of the contact area. Among the three variants of the model, the worst predictions (those differing most from the experiment) are produced when collagen

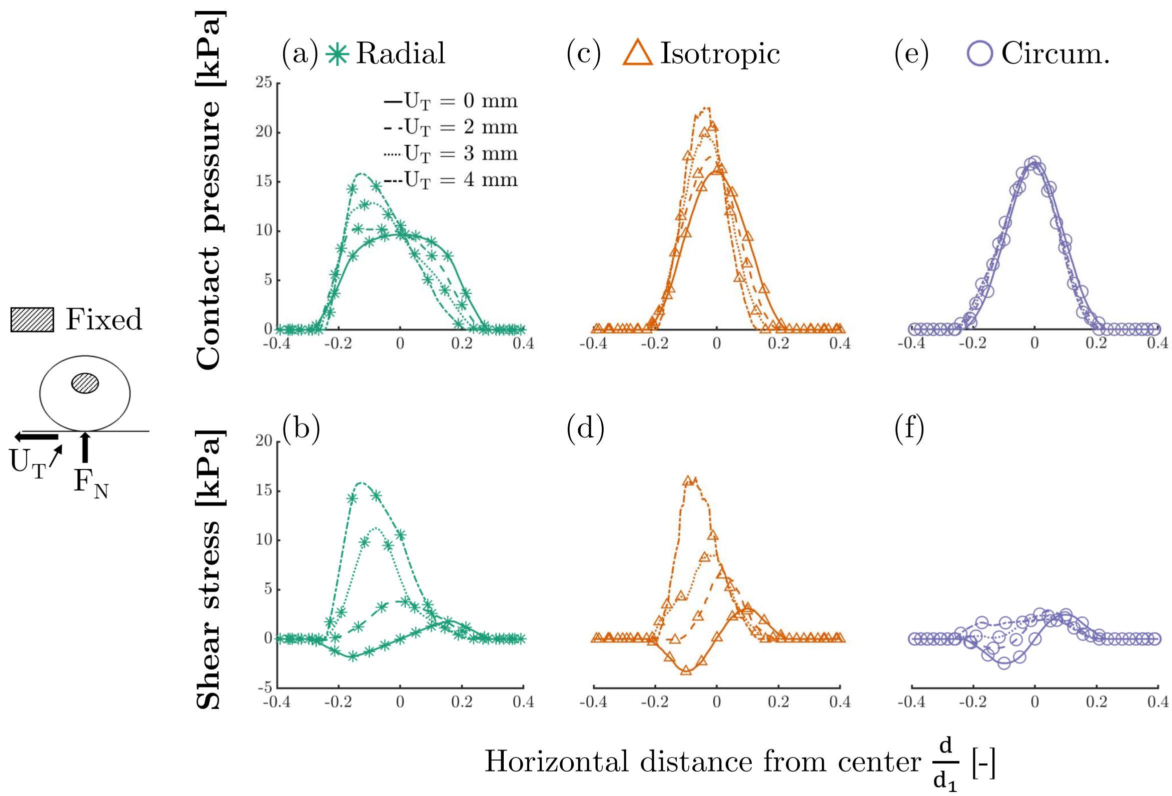

Fig. 4. Evolution of the pressure and shear stress along the contact line between fingertip and rigid surface. The pressure profile is symmetric and the shear stress distribution is skew-symmetric under pure normal load $F_N = 0.5$ N (continuous lines). When contact involves both normal force and tangential displacement (i.e., $U_T > 0$ mm), the maximum pressure is progressively shifted to the trailing side of the finger. Symbols represent a fraction of the extracted data points value.

fibers are circumferentially aligned. The variant of the model with radial fibers is the one performing best, in particular with regard to the predicted contact area under sliding. The variant with circumferential fibers is the only one exhibiting excessive "rolling" phenomenon, i.e., the circumferential motion of the skin relative to the bone induced by friction with the plate under tangential loading.

According to Fig. 3(c) and (d), full slip occurs at a tangential displacement of ∼4 mm and ∼5 mm for the variants which consider, respectively, radial and random fiber orientations. Figure 4 shows how the profiles of pressure and shear stress predicted along the line of contact at the glass-fingertip interface evolve before full slip. These profiles are obtained after using the *smooth* function in Matlab with a moving average window of size 20. The solid lines correspond to the predictions after normal loading, whereas the profiles represented with dashed lines, dotted lines and dashed-dotted lines refer to predictions after a tangential displacement U_T of, respectively, 2 mm, 3 mm and 4 mm. After normal loading (when $U_T = 0$ mm), the variant of the model with a radial fiber network predicts a contact pressure with a flattened bell profile, whereas the circumferential and isotropic networks of collagen fibers lead to Hertzian profiles with higher amplitudes. When tangential displacement increases, the pressure profiles become asymmetric and the peak amplitude is shifted towards the trailing edge of the fingertip. The transition is most sudden in case of the radial fiber network and much more subtle in case of circumferentially oriented fibers. Similar observations are made when considering the profiles of contact shear stress.

Figure 5 shows how the anisotropy of the mechanical response influences the heterogeneous deformation of subcutaneous tissues. The deformation fields, measured when the imposed 8 mm tangential displacement is reached, are analyzed by mapping two variables λ_r and λ_θ, which correspond to the local material stretch along, respectively, the radial and circumferential directions. Values larger and lower than 1 correspond, respectively to elongation and contraction along the given direction. In these subfigures, which compare the different variants of the model, we may notice that stretches are impeded

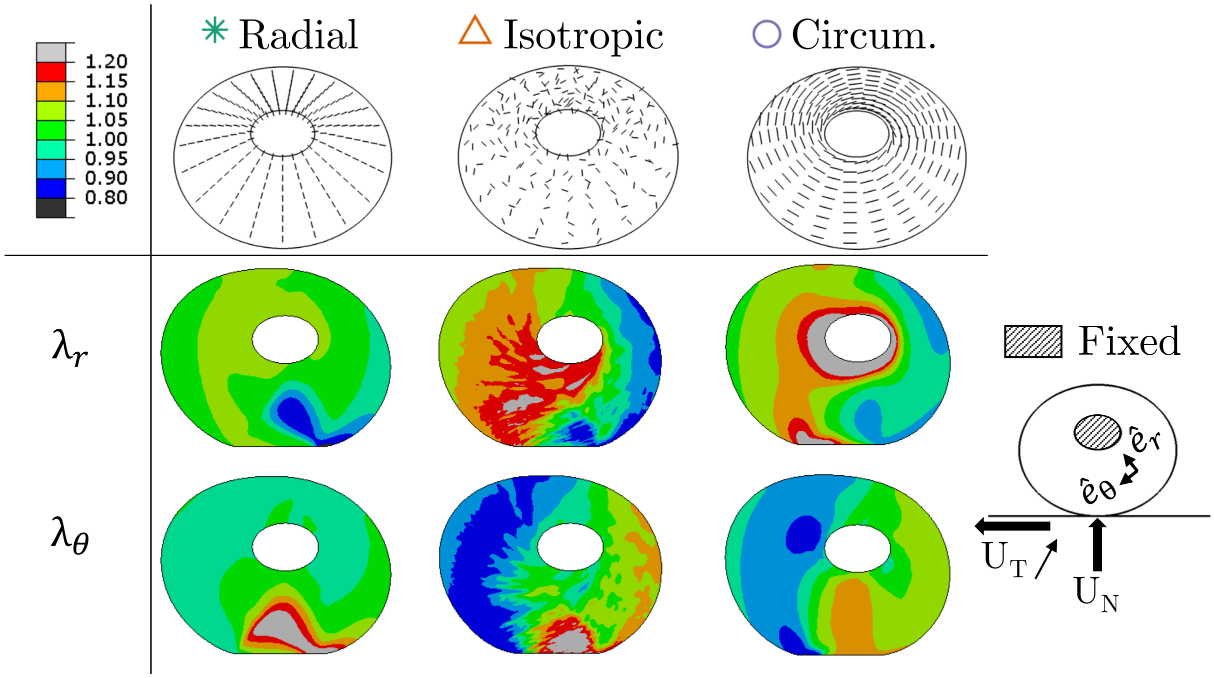

Fig. 5. Elongation or contraction λ_r and λ_θ of the material along, respectively, the radial $\hat{\mathbf{e}}_r$ and circumferential $\hat{\mathbf{e}}_\theta$ local directions. In the three simulations (involving different networks of collagen fibers), the contact of the finger with the plate involves normal displacement U_N of 1 mm and a tangential displacement U_T of 8 mm.

(or at least hindered) in the direction of collagen fibers. For instance, the connection of the soft tissues to the bone is stiffer in the case of the radial network of fibers (the values of λ_r around the bone are lowest with this variant of the model).

V. Discussion

The development of haptic devices requires a thorough understanding of the physiological processes likely to explain the sense of touch. The present study demonstrates that, when a fingertip is pressed against a surface, the anisotropy of subcutaneous tissues greatly influences the strain and stress fields in the neighborhood of the tactile afferents that trigger neuronal activity. According to the model, the local stretches experienced by such biological sensors vary greatly, depending on the orientations of the network of collagen fibers (Fig. 5). Radial fiber networks, as observed in histological observations, prevent the ”rolling” phenomenon (Fig. 3) and also induce a sudden change of the contact pressure and shear stress (Fig. 4) early in the transition from sticking to slipping. This likely has major impact on tactile feedback. Indeed, tactile afferents are considered highly sensitive to the local pressure and to its rate of change [2]. The occurrence of an asymmetric pressure profile before full slip might be a crucial feedback in order to maintain a stable grasp during manipulation [3]. However, there is a current lack of research on non-invasive feedback designs for slip sensations [35]. Wearable technologies, like haptic gloves, often rely on pneumatic actuation to provide sensory feedback [36] and it has been shown that static pressure alone can be used to enable slip detection [37]. Still, better performances were obtained when relying on vision or vibrotactile feedback. The results of this study might suggest that haptic feedback based on dynamic pressure could efficiently convey slippage information. Incorporating reliable feedback for slippage into haptic gloves could improve the immersion of the interactions with the AR/VR environments.

The model proposed here relies on some highly simplifying assumptions but its predictions are realistic. Experimental measurements of the load-displacement curve and the evolution of the contact area of a fingerpad pressed on a rigid surface are properly reproduced. This is achieved by using model parameter values in the same range as those identified in many other studies using the HGO model to compute the response of soft biological tissues. The numerical predictions are closest to experimental trends when the orientation of collagen fibers corresponds to histological observations whereas the circumferential and isotropic variants of the model underestimate the increase of the contact area (Fig. 3(b)). Similarly, classic isotropic hyperelastic models, such as those used in Reference 1 and Reference 2, greatly underestimate the evolution of the contact area (Fig. 3(b)) even when considering more realistic multi-layered 3D geometries. Notably, the angles of attack used in these reference models (i.e., 15° and 20°, respectively) are smaller than the angle of attack used in the experimental data (i.e., 30°). Moreover, studies have shown that larger contact areas are achieved at smaller angles of attack (see Fig. 1(b) or [26]). Consequently, the 3D models featured in Reference 1 and in Reference 2 should theoretically predict a contact area even greater than what is observed in the experimental data utilized in this study. Thus, given the discrepancy in angles of attack between the experimental data and the reference models, their underestimation of the contact area is notably exacerbated. As collagen fibers sustain much better axial elongation (tensile stresses) than compression, the physiological fiber configuration, i.e., the radial network, lowers the macroscopic stiffness under compression along the main direction of loading (normal to the rigid surface). This accelerates the growth of the contact area, flattening the profile of contact pressure. The latter has so far not been studied in great detail experimentally, but the available data shows similar trends [1].

The numerical simulations are here performed in 2D, while assuming a uniform strain in the out-of-plane direction, i.e., generalized plane strain. In the present study, it was observed that the amplitude of the out-of-plane deformation does not influence the main trends in the numerical results. The 2D assumption seems justified given the in-plane distribution of collagen fiber orientations and the fact that the finger in contact with the plate moves along a direction parallel to the cross-section that is modeled (Fig. 1). The selected 2D model demonstrates at reduced computational cost the significance of the anisotropy induced by the network of collagen fibers on the biomechanics of the fingertip. However, the simulation of more general loading scenarios would require adapting the model from 2D to 3D. This will, for instance, enable to study the impact of the angle of attack on the mechanical response of the fingertip which can not be captured by the current 2D model. Experimental campaigns justifying such 3D modeling are still under progress [3].

In the present study, the viscoelastic properties of the subcutaneous tissues have been neglected. However, it has been shown that the load-displacement response of the fingertip exhibits stiffer behavior at higher loading rates [38]. Viscous effects could impact locally the deformations predicted in Fig. 5 as some regions within the fingertip might deform faster than others. Nevertheless, these effects should not change the trends in term of the anisotropy induced by the network of collagen fibers as the traction/contraction asymmetry of collagen is independent of viscosity. Including viscous effects would allow to explore the response of the fingertip under dynamic situations of spontaneous tactile exploration.

The model could also be enhanced by including the nail. The latter is known to influence both the gripping and sensing capabilities of the fingertip [39] and is a source of anisotropy as well. However, unlike collagen fibers, the nail has been considered in previous modeling of the fingertip [11], [16]. Still, it could be interesting to investigate how these two sources of anisotropy contribute to the global fingertip response in a 3D model.

Another potential improvement of this work would be to account for the heterogeneity of subcutaneous tissues [15], [16]. In this work, the material response is considered homogeneous apart from the local orientation of collagen fibers. In reality, not only the orientation but also the density of collagen fibers varies from place to place, with the highest fiber density under the nail. The present model also disregards the layered structure of the skin itself. The outermost viable epidermis and dermis are stiffer than the subcutaneous tissues, thus forming a thin “membrane” which is likely to have some influence on the local stress and strain fields. The biological mechanoreceptors are located at the junction between the viable epidermis and the dermis. More precisely, Merkel cells (associated with SA-I afferents) are found at the tip of inner ridges (mirroring the fingerprint ridges) and Meissner corpuscles (associated with FA-I afferents) are nested inside the dermal papillae [40], [41]. Such arrangement surely pursues a goal and it motivates the development of a microscale modeling complementing the present one.

VI. Conclusion

The mechanical anisotropy of subcutaneous tissues has a major influence on both the distribution of contact stresses and the overall deformation of a fingerpad under normal and tangential loading. This is a direct consequence of the nonlinear and directional stiffening of stretched collagen fibers. In the present study, the predictions of a two-dimensional FE model are compared to experimental observations of a fingerpad pressed on a rigid surface, leading to the following conclusions:

- As compared to two alternative modeling hypotheses, the laboratory experiments are reproduced most accurately using the model variant which considers physiological orientations of collagen fibers (radial network).

- The pressure profile along the line of contact of the fingerpad with the surface has a realistic flattened bell shape when collagen fibers are oriented radially and this pressure profile changes suddenly in the transition from sticking to slipping. The latter is likely to produce efficient feedback when grasping objects.
- The mechanical anisotropy induced by the collagen fibers influences also the deformation in the close neighborhood of the tactile afferents triggering neuronal activity. This should be accounted for in the development of haptic devices.

Acknowledgments

LD and BD are mandated by the Belgian National Fund for Scientific Research (FSR-FNRS).

References

[1] R. S. Johansson and J. R. Flanagan, "Coding and use of tactile signals from the fingertips in object manipulation tasks," *Nature Reviews Neuroscience*, vol. 10, no. 5, pp. 345–359, 2009.

[2] K. O. Johnson, "The roles and functions of cutaneous mechanoreceptors," *Current opinion in neurobiology*, vol. 11, no. 4, pp. 455–461, 2001.

[3] B. P. Delhaye, E. Jarocka, A. Barrea, J.-L. Thonnard, B. Edin, and P. Lefevre, "High-resolution imaging of skin deformation shows that afferents from human fingertips signal slip onset," *Elife*, vol. 10, e64679, 2021.

[4] J. R. Phillips and K. O. Johnson, "Tactile spatial resolution. III. A continuum mechanics model of skin predicting mechanoreceptor responses to bars, edges, and gratings," *Journal of neurophysiology*, vol. 46, no. 6, pp. 1204–1225, 1981.

[5] A. P. Sripati, S. J. Bensmaia, and K. O. Johnson, "A continuum mechanical model of mechanoreceptive afferent responses to indented spatial patterns," *Journal of neurophysiology*, vol. 95, no. 6, pp. 3852–3864, 2006.

[6] H. P. Saal, B. P. Delhaye, B. C. Rayhaun, and S. J. Bensmaia, "Simulating tactile signals from the whole hand with millisecond precision," *Proceedings of the National Academy of Sciences*, vol. 114, no. 28, E5693–E5702, 2017.

[7] M. A. Srinivasan, "Surface deflection of primate fingertip under line load," *Journal of biomechanics*, vol. 22, no. 4, pp. 343–349, 1989.

[8] M. Srinivasan and K. Dandekar, "An investigation of the mechanics of tactile sense using two-dimensional models of the primate fingertip," *Journal of biomechanical engineering*, vol. 118, no. 1, pp. 48–55, 1996.

[9] J. Z. Wu, D. E. Welcome, K. Krajnak, and R. G. Dong, "Finite element analysis of the penetrations of shear and normal vibrations into the soft tissues in a fingertip," *Medical engineering & physics*, vol. 29, no. 6, pp. 718–727, 2007.

[10] K. Dandekar, B. I. Raju, and M. A. Srinivasan, "3-D finite-element models of human and monkey fingertips to investigate the mechanics of tactile sense," *J. Biomech. Eng.*, vol. 125, no. 5, pp. 682–691, 2003.

[11] G. J. Gerling and G. W. Thomas, "Fingerprint lines may not directly affect SA-I mechanoreceptor response," *Somatosensory & motor research*, vol. 25, no. 1, pp. 61–76, 2008.

[12] G. Harih and M. Tada, "Finite element evaluation of the effect of fingertip geometry on contact pressure during flat contact," *International journal for numerical methods in biomedical engineering*, vol. 31, no. 6, 2015.

[13] G. Harih, M. Tada, and B. Dolšak, "Justification for a 2D versus 3D fingertip finite element model during static contact simulations," *Computer methods in BiomeChaniCs and BiomediCal engineering*, vol. 19, no. 13, pp. 1409–1417, 2016. DOI: 10.1080/10255842.2016.1146712.

[14] C. Wex, S. Arndt, A. Stoll, C. Bruns, and Y. Kupriyanova, "Isotropic incompressible hyperelastic models for modelling the mechanical behaviour of biological tissues: A review," *Biomedical Engineering/Biomedizinische Technik*, vol. 60, no. 6, pp. 577–592, 2015.

[15] J. Z. Wu, K. Krajnak, D. E. Welcome, and R. G. Dong, "Three-Dimensional Finite Element Simulations of the Dynamic Response of a Fingertip to Vibration," *Journal of Biomechanical Engineering*, vol. 130, no. 5, p. 054 501, 2008.

[16] G. Serhat and K. J. Kuchenbecker, "Free and forced vibration modes of the human fingertip," *Applied Sciences*, vol. 11, no. 12, p. 5709, 2021.

[17] R. M. Hauck, L. Camp, H. P. Ehrlich, G. C. Saggers, D. R. Banducci, and W. P. Graham, "Pulp nonfiction: Microscopic anatomy of the digital pulp space," *Plastic and reconstructive surgery*, vol. 113, no. 2, pp. 536–539, 2004.

[18] C. H. Daly, "Biomechanical properties of dermis," *Journal of Investigative Dermatology*, vol. 79, no. 1, pp. 17–20, 1982.

[19] T. C. Gasser, R. W. Ogden, and G. A. Holzapfel, "Hyperelastic modelling of arterial layers with

distributed collagen fibre orientations," *Journal of the royal society interface*, vol. 3, no. 6, pp. 15–35, 2006.

[20] L. Dorfmann and R. W. Ogden, *Nonlinear mechanics of soft fibrous materials*. Springer, 2015. DOI: 10.1007/978-3-7091-1838-2.

[21] D. Doumont, A. Kao, G. Gerling, A. Browet, B. Delhaye, and P. Lefèvre, "3-D reconstruction of the fingertip deformation during tactile interactions," in *Worldhaptics Annual Meeting*, 2023.

[22] C. A. Schneider, W. S. Rasband, and K. W. Eliceiri, "Nih image to imagej: 25 years of image analysis," *Nature methods*, vol. 9, no. 7, pp. 671–675, 2012.

[23] Dassault Systèmes, "Simulia user assistance 2021: Abaqus," https://help.3ds.com/2021/english/DSSIMULIA_Established/SIMULIA_Established_FrontmatterMap/sim-r-DSDocAbaqus.htm?contextscope=all&id=b15ba98a76ce4305b417ecdd54e5394d (accessed April 8, 2024).

[24] C. Geuzaine and J.-F. Remacle, "Gmsh: A 3-D finite element mesh generator with built-in pre- and post-processing facilities," *International journal for numerical methods in engineering*, vol. 79, no. 11, pp. 1309–1331, 2009.

[25] D. S. Bombarde, L. N. Silla, S. S. Gautam, and A. Nandy, "A comprehensive comparative review of various advanced finite elements to alleviate shear, membrane and volumetric locking," *Archives of Computational Methods in Engineering*, pp. 1–35, 2024.

[26] B. M. Dzidek, M. J. Adams, J. W. Andrews, Z. Zhang, and S. A. Johnson, "Contact mechanics of the human finger pad under compressive loads," *Journal of The Royal Society Interface*, vol. 14, no. 127, p. 20 160 935, 2017.

[27] B. P. Delhaye, P. Lefevre, and J.-L. Thonnard, "Dynamics of fingertip contact during the onset of tangential slip," *Journal of The Royal Society Interface*, vol. 11, no. 100, p. 20 140 698, 2014.

[28] D. Drevon, S. R. Fursa, and A. L. Malcolm, "Intercoder reliability and validity of webplotdigitizer in extracting graphed data," *Behavior modification*, vol. 41, no. 2, pp. 323–339, 2017.

[29] MATLAB, *Version 9.10.0.1851785 (R2021a) Update 6*, Natick, Massachusetts: The Mathworks, Inc., 2021.

[30] A. M. Smith, G. Gosselin, and B. Houde, "Deployment of fingertip forces in tactile exploration," *Experimental brain research*, vol. 147, pp. 209–218, 2002.

[31] E. Battaglia, M. Bianchi, M. L. D'Angelo, M. D'Imperio, F. Cannella, E. P. Scilingo, and A. Bicchi, "A finite element model of tactile flow for softness perception," in *2015 37th Annual International Conference of the IEEE Engineering in Medicine and Biology Society (EMBC)*, IEEE, 2015, pp. 2430–2433.

[32] J. Dallard, S. Duprey, and X. Merlhiot, "Simplified versus real geometry fingertip models: A finite element study to predict force–displacement response under flat contact compression," *Journal of Mechanics in Medicine and Biology*, vol. 18, no. 04, p. 1 850 048, 2018.

[33] D. Chamoret, F. Peyraut, S. Gomes, and Z.-Q. Feng, "Finite element approach applied to human digital model for biomechanical modeling," *International Journal on Interactive Design and Manufacturing (IJIDeM)*, vol. 4, no. 1, pp. 75–82, 2010.

[34] J. van Kuilenburg, M. A. Masen, and E. van der Heide, "A review of fingerpad contact mechanics and friction and how this affects tactile perception," *Proceedings of the Institution of Mechanical Engineers, Part J: Journal of engineering tribology*, vol. 229, no. 3, pp. 243–258, 2015.

[35] J. M. Walker, A. A. Blank, P. A. Shewokis, and M. K. O'Malley, "Tactile feedback of object slip facilitates virtual object manipulation," *IEEE transactions on haptics*, vol. 8, no. 4, pp. 454–466, 2015.

[36] J. Yin, R. Hinchet, H. Shea, and C. Majidi, "Wearable soft technologies for haptic sensing and feedback," *Advanced Functional Materials*, vol. 31, no. 39, p. 2 007 428, 2021.

[37] M. R. Motamedi, J.-B. Chossat, J.-P. Roberge, and V. Duchaine, "Haptic feedback for improved robotic arm control during simple grasp, slippage, and contact detection tasks," in *2016 IEEE International Conference on Robotics and Automation (ICRA)*, IEEE, 2016, pp. 4894–4900.

[38] D. T. V. Pawluk and R. D. Howe, "Dynamic Lumped Element Response of the Human Fingerpad," *Journal of Biomechanical Engineering*, vol. 121, no. 2, pp. 178–183, 1999.

[39] K. Sakuma, A. Abrami, G. Blumrosen, S. Lukashov, R. Narayanan, J. W. Ligman, V. Caggiano, and S. J. Heisig, "Wearable nail deformation sensing for behavioral and biomechanical monitoring and human-computer interaction," *Scientific reports*, vol. 8, no. 1, p. 18 031, 2018.

[40] G. J. Gerling, "SA-I mechanoreceptor position in fingertip skin may impact sensitivity to edge stimuli," *Applied Bionics and Biomechanics*, vol. 7, no. 1, pp. 19–29, 2010.

[41] T. Maeno, K. Kobayashi, and N. Yamazaki, "Relationship between the structure of human fin-

ger tissue and the location of tactile receptors," *JSME International Journal Series C Mechanical Systems, Machine Elements and Manufacturing*, vol. 41, no. 1, pp. 94–100, 1998.